JOURNAL OF MATERIALS SCIENCE 25 (1990) 4525–4530

Effect of gadolinium content on the thermal volume change of $Ba_4Na_2Nb_{10}O_{30}$–$Ba_3NaGdNb_{10}O_{30}$ solid solutions at ferroelectric phase transition temperature

M. SHIMAZU, M. TSUKIOKA
National Institute for Research in Inorganic Materials 1-1 Namiki, Tsukuba-Shi, Ibaraki 305, Japan

N. MITOBE, S. KUROIWA, S. TSUTSUMI
School of Science and Engineering, Waseda University, 3-4-1 Ookubo, Shinjuku-Ku, Tokyo 160, Japan

For sintered samples of $Ba_{3+x}Na_{1+x}Gd_{1-x}Nb_{10}O_{30}$ ($1 \geqslant x \geqslant 0$), the effect of the addition of gadolinium to barium sodium niobate (BNN, $x = 1$, tungsten bronze type) was examined by differential scanning calorimetry (DSC) and X-ray powder diffractometry. The volume change (i.e. especially the change of c-axis length) at the ferroelectric phase transition temperature ($T_c < 590°C$) decreased with the increasing gadolinium content. This result suggests that the addition of gadolinium or other lanthanide elements to BNN is possibly effective to obtain an uncracked single crystal with the Czochralski technique. The DSC indicator method is useful to determine the relative magnitude of volume change at T_c for the same type of sample series, a method which is much easier than the dilatometer method. The relation between the DSC peak area and the volume change of unit cell at T_c is discussed from the thermodynamic viewpoint.

1. Introduction

Barium sodium niobates (BNN) having a tungsten bronze type of structure [1] are well known as ferroelectric and optically nonlinear materials (Table I). However, their optoelectronic application has not been made industrially because high quality of the single crystal or thin film has not yet been achieved.

The greatest difficulty in producing a good quality BNN single crystal by the Czochralski (Cz) technique is due to the large thermal expansion of the c-axis at temperatures in the range 590 to 520° C during cooling after crystal growth [4]. On passing through this temperature, the crystal suffers cracking. Microtwins occur on the tetragonal to orthorhombic phase transition below 300° C [2]. This microtwinning can be suppressed by a cooling procedure under an applied stress (for example, 100 or 200 $kg\,cm^{-2}$) from a temperature above 300° C down to room temperature [3]. The microtwins disturb the optically second harmonic generation (SHG) effect. However, the occurrence of cracking at the ferroelectric phase transition (about 580° C) is the most serious problem.

Mukherjee *et al.* [14] reported that the substitution of gadolinium for the barium and sodium in BNN is effective in depressing the outstanding thermal expansion.

In the present paper, for samples of $Ba_4Na_2Nb_{10}O_{30}$ (BNN)-$Ba_3NaGdNb_{10}O_{30}$ (BNGN) solid solution, the gadolinium effect on the volume change at the ferroelectric phase transition is examined by differential scanning calorimetry (DSC) and X-ray diffraction. Two of our samples have the same compositions as those of Mukherjee.

2. Experimental procedure and results

2.1. Sample preparation

In the pseudobinary system of BNN–BNGN, as shown in Table II, eleven kinds of solid solution were prepared, where the BNN–BNGN solid solutions are represented by the formula xBNN · $(1 - x)$ BNGN, or $Ba_{3+x}Na_{1+x}Gd_{1-x}Nb_{10}O_{30}$, $(1 \geqslant x \geqslant 0)$. In Table II, for example B6G4 indicates the solid solution of 0.6 BNN · 0.4 BNGN, where the atomic ratio of Ba/Na/Gd is 3.6/1.6/0.4. The ratio of Nb/O = 10/30 is maintained in all samples.

The starting chemicals are $BaCO_3$, Na_2CO_3 (Shoowa-Kagako-Koogyo Co.), Gd_2O_3 (Rar Metallic Co.), and Nb_2O_5 (Hermann-Stark Co.) powders all of which are 99.99% chemically pure. On weighing, the humidity of the chemicals was taken into consideration and each chemical was weighed to suppress error to within 0.01%. However, the humidity-absorption of Na_2CO_3 was noticeable and so it was necessary for the chemicals to be kept in a drier with a certain humidity and weighed quickly.

The chemicals were mixed homogeneously and pressed under 150 $kg\,cm^{-2}$ to form pellets of 16 mm diameter. The pellets were heated and sintered in air at

0022–2461/90 $03.00 + .12

TABLE I Phases of barium sodium niobate (BNN) [1–13]

	Phase				
	IV	III	INC	II	I
State	ferroelec. paraelastic	ferroelec. ferroelastic		ferroelec. paraelastic	paraelec. paraelastic
Crystal system	tetragonal	orthorhombic		tetragonal	tetragonal
Space group	P4bm (No. 100)	Cmm2 (No. 35)		P4bm (No. 100)	P4/mbm (No. 127)
Point group	4mm	mm2		4mm	4/mmm
Symmetry	noncentro.	noncentro.		noncentro.	centro.
Trans. temp. (°C)	(about)	−163	250	284	570
Phase transition			(INC) ferroelastic-trans.	(INC)	ferroelec.-trans.

INC: incommensurate phase (transition).
Trans. temp.: phase transition temperature.

about 1150° C for 12 h. The heating procedure with pulverizing and pressing was repeated three or four times in order to obtain homogeneous material. When homogeneity was attained, the X-ray diffraction patterns or lattice parameters were found to be unchanged compared with a previously synthesized sample.

2.2. Room-temperature X-ray diffraction measurements

The X-ray powder diffraction pattern of a stoichiometric BNN is shown in Fig. 1. The Miller indices ($h\,k\,l$) are correctly assigned as a pseudotetragonal symmetry. The details of assignment will be reported elsewhere [17].

As shown in Fig. 2, with increasing gadolinium content, the doublets of (0 0 2), (2 4 0), and (0 4 2), (0 6 0) appear as a single peak, respectively. Thus $d(0\,0\,2) = d(2\,4\,0)$ and $d(0\,4\,2) = d(0\,6\,0)$, i.e. $a = 5^{1/2}c$ in pseudotetragonal symmetry. As seen in Fig. 3, the c-axis length decreases with increasing gadolinium content while the a-axis length increases very slightly. The decrease in the c-axis is remarkable in the range between BNN and B4G6.

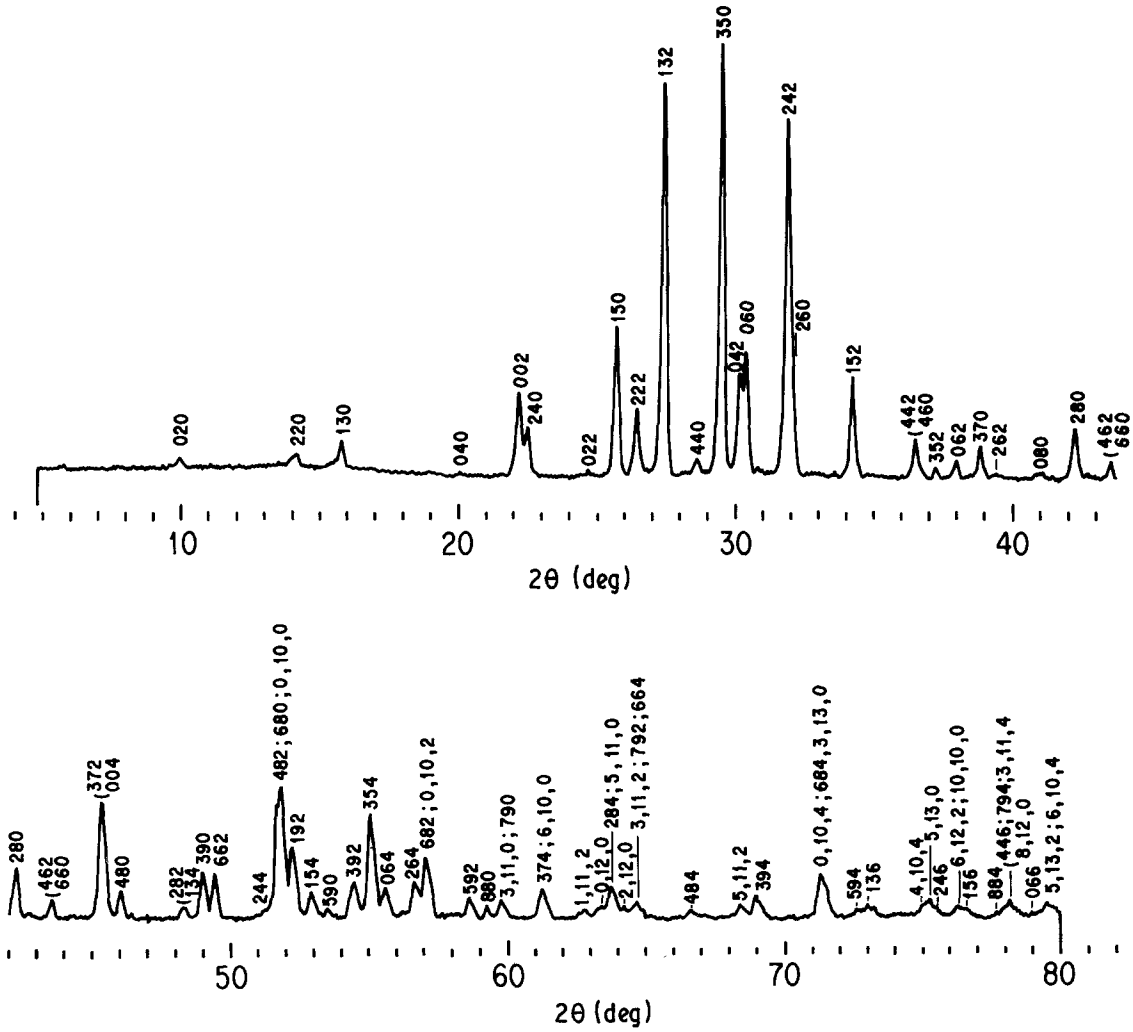

Figure 1 X-ray powder diffraction pattern of a stoichiometric $Ba_4Na_2Nb_{10}O_{30}$ (BNN-S) sample. The powder sample was mounted such that it did not have the preferred orientation of powder particles. Pseudo-tetragonal, $a = b = 1.759\,94\,(8)$ nm, $c = 0.799\,71\,(9)$ nm. Cu$K\alpha$, nickel filtered, 35 kV, 16 mA. 1°–0.3–1°, $f = 4000$ c.p.s., $t = 2$ sec, scanning speed 2° min^{-1}, Rigaku Denki X-ray diffractometer.

TABLE II The samples

Sample	Composition	Atomic ratio			
		Ba	Na	Gd	Gd/(Ba + Na) (%)
BNN	$Ba_4Na_2Nb_{10}O_{30}$	4.0	2.0	0.0	0.00
B9G1	0.9 mol BNN + 0.1 mol BNGN	3.9	1.9	0.1	1.72
B8G2	0.8 + 0.2	3.8	1.8	0.2	3.57
B7G3	0.7 + 0.3	3.7	1.7	0.3	5.55
B6G4	0.6 + 0.4	3.6	1.6	0.4	7.69
B5G5	0.5 + 0.5	3.5	1.5	0.5	10.00
B4G6	0.4 + 0.6	3.4	1.4	0.6	12.50
B3G7	0.3 + 0.7	3.3	1.3	0.7	15.21
B2G8	0.2 + 0.8	3.2	1.2	0.8	18.18
B1G9	0.1 + 0.9	3.1	1.1	0.9	21.42
BNGN	$Ba_3NaGdNb_{10}O_{30}$	3.0	1.0	1.0	25.00

General formula: xBNN–$(1 - x)$ BNGN, or $Ba_{3+x}Na_{1+x}Gd_{1-x}NB_{10}O_{30}$, $(1 \geqslant x \geqslant 0)$.

In the tungsten bronze-type crystal structure [1], the pentagonal tunnel sites are occupied predominantly by Ba^{2+} ions while the square tunnel sites are occupied predominantly by Na^+ and Gd^{3+} ions. According to Shannon and Prewitt [16], the ionic radii are 0.136 nm for Ba^{2+} (VI), 0.102 nm for Na^+ (VI), and 0.0938 nm for Gd^{3+} (VI), respectively. The coordination number in the BNN-BNGN structure is different from VI, but the size of its ionic radius may be comparable. Thus it is possible that the Gd^{3+} ion prefers the square sites to the pentagonal sites. The framework constructed by NbO_6 octahedra is strongly combined at the *ab*-axes plane level, and so it is natural that the $a(=b)$-axis length can be retained without large variation in spite of the different ratios of Gd/(Ba + Na). On the other hand, the *c*-axis length parallel to the "open" tunnel may easily suffer changes with variation of the atomic ratio. Because the Gd^{3+} ion has the smallest ionic size, the *c*-axis becomes smaller with the increasing Gd/(Ba + Na).

It can be supposed that this aspect of the thermal volume change of the lattice on the ferroelectric phase transition is more or less different between the low gadolinium content samples and the high gadolinium content samples, the boundary of which is B4G6 (Fig. 3).

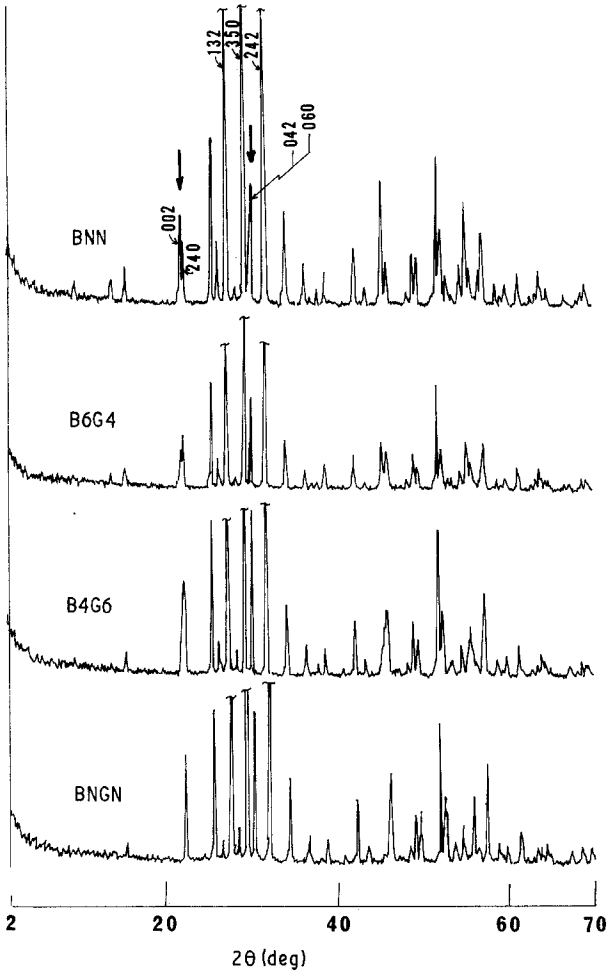

Figure 2 X-ray powder diffraction patterns of the BNN–BNGN solid solutions (see Table II).

2.3. Differential scanning calorimetric (DSC) measurements

Assuming that the height of the DSC endothermal peak at the ferroelectric phase transition temperature (T_c) reflects the volume change at that temperature, DSC measurements were attempted. The thermodynamic discussion based on this assumption is presented in Section 3.

The conditions for DSC measurement are given in Table III, and the DSC curves are shown in Fig. 4. The weights of the samples are slightly different, as shown in Table IV. It is, however, obvious that both the area (A_c) and peak temperature (T_c) of the endothermal peak decrease with increasing gadolinium content. The peak cannot be detected for samples of high gadolinium content, such as B4G6, etc., and BNGN. This boundary (B4G6) at which the peak disappears agrees with that of *c*-axis variation at room temperature (Fig. 3).

It is known that the DSC peak area (A_c) corresponds to the transition enthalpy (ΔH_c), where $\Delta H_c = kA_c$ (k is a conversion factor). The transition enthalpy of quartz at 573° C was reported to be 0.174 kcal mol^{-1} [15]. ΔH_c of BNN–BNGN samples

TABLE III Conditions for DSC measurements (see Fig. 4)

Temperature sensor	K(CA)-type thermocouple
DSC range	1 mcal sec^{-1}
Reference	α-Al_2O_3
Heating rate	10° C min^{-1}
Chart speed	5 mm min^{-1}
Atmosphere	N_2 gas flow
Sample holder	Pt pan (5 mm diameter, 2.5 mm high)

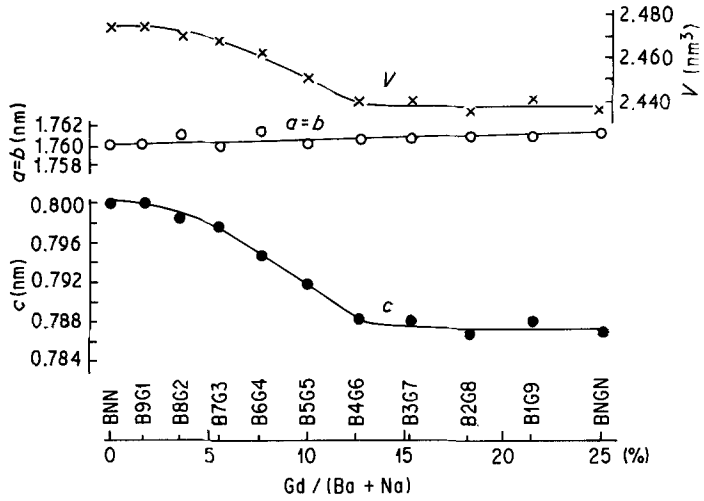

Figure 3 Vaiations of the lattice parameters (a and c) and the volume (V) of the unit cell at room temperature in the BNN–BNGN solid solutions.

can be calculated by comparing the peak area of the sample with that of quartz. Although the definition of peak area in Fig. 4 is difficult, approximate values of A_c and ΔH_c are shown in Table IV. The results show that T_c and ΔH_c decrease with increasing gadolinium content or Gd/(Ba + Na) ratio.

It is now expected that the larger the value of ΔH_c, the larger will be the thermal volume change of the unit cell at T_c.

2.4. High-temperature X-ray diffraction measurements

In order to confirm the validity of the assumption, for our samples, that the size of DSC peak area (and so ΔH_c) corresponds to the magnitude of the volume change of a unit cell at T_c, the change in lattice parameters with temperature was measured. The lattice parameters $a(=b)$ and c were calculated from the observed lattice spacings of (1 3 2) (3 5 0) (2 4 2) diffractions (Fig. 1). The accuracy of measurement with the high-temperature X-ray diffractometer was not good. Therefore, the spacings were corrected by comparing with data at room temperature which were obtained using another X-ray diffractometer. The results are shown in Figs 5 and 6. The change in a-axis length between the samples is not distinctive, while that of the c-axis is characteristic. The magnitude of thermal contraction ($\Delta c/c$, or $\Delta v/v$) in the range of 400 to 600° C becomes smaller with increasing gadolinium content. This result correlates to the variation in ΔH_c, and it justifies the assumption that the DSC peak area reflects the volume change of the unit cell at T_c.

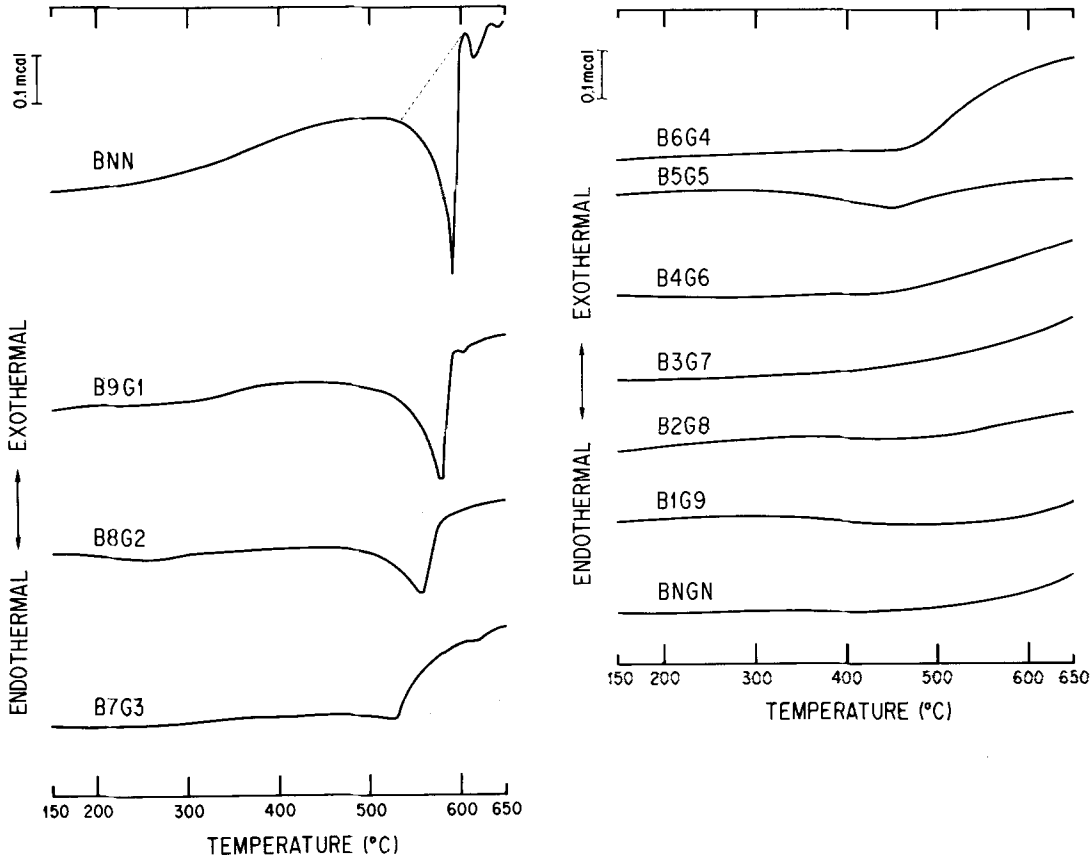

Figure 4 Differential scanning calorimetry (DSC) curves of the BNN–BNGN solid solutions (see Tables III and IV).

TABLE IV Enthalpy (ΔH_c) of the ferroelectric phase transition (see Fig. 4)

Sample	Weight (mg)	Temp. T_c (°C)	Peak area, A_c (mm^2)	Enthalpy, ΔH_c (kcal mol^{-1})
BNN	95.79	587	2246.464	2.674
B9G1	88.23	572	1117.536	1.444
B8G2	89.64	554	673.619	0.857
B7G3	96.51	528		
B6G4	98.54	465		
B5G5	96.80	452		
B4G6	95.96			
B3G7	96.66			
B2G8	92.33			
B1G9	95.20			
BNGN	97.40	20 [8]		
		The others could not be measured		

The enthalpy of the phase transition of low- to high-form quartz at 573° C is 0.174 kcal mol^{-1} [15].
Weight: sample weight.
T_c: temperature of ferroelectric transition.
A_c: endothermal peak area at T_c.
ΔH_c: enthalpy of the phase transition at T_c.

3. Discussion

The problem of the correspondence of the DSC peak area to the volume change of a unit cell at phase transition temperature is now discussed.

The model of the thermodynamic relationship of the phase transition is drawn in Fig. 7. Suffix 1 indicates a high-temperature form of the phase and suffix 2 the low-temperature form. The phase transition occurs at a temperature T_c. The following formulae are well known

$$G = H - TS \quad (1)$$

$$(\partial G/\partial T)_p = -S, \quad (H = E + PV) \quad (2)$$

where G is the Gibbs' free energy, H the enthalpy, T the absolute temperature, S the entropy, E the internal energy, P the pressure and V the volume. If the transition has a sharp critical point, it becomes $G_1 = G_2$ at T_c. Then

$$\Delta H_c = T_c \Delta S_c, \quad (\Delta H = H_1 - H_2, \Delta S = S_1 - S_2) \quad (3)$$

$$\Delta S_c \neq 0 \quad (4)$$

The phase transition of $\Delta S_c \neq 0$ is termed the first order of the phase transition, and thus $\Delta H_c \neq 0$.

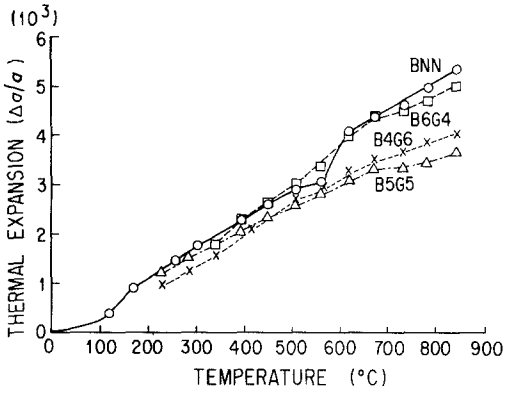

Figure 5 Linear thermal expansion of the a-axis in the BNN–BNGN solid solutions. Measurements were made by high-temperature X-ray diffraction. Δa indicates the thermal change in the length of the a-axis.

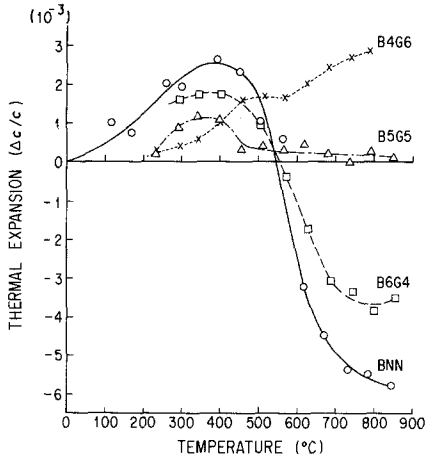

Figure 6 Linear thermal expansion of the c-axis in the BNN–BNGN solid solutions. Measurements were made by high-temperature X-ray diffraction. Δc indicates the thermal change in the length of the c-axis.

Any ferroelectric phase transition belongs to the "displacive type" of phase transition. ΔH_c of the ferroelectric phase transition occurs due to various factors, namely, volume change (and so the shift of atomic positions), domain change, etc. In DSC measurement, it is proved that the endothermal peak area (A_c) corresponds to the enthalpy (ΔH_c) where $\Delta H_c = kA_c$ (see Section 2.3). When the volume change between phases 1 and 2 is large, the magnitude of ΔH_c is comparable to the volume change. When the entropies, namely the gradients of the G curves, intersect sharply at T_c, a sharp DSC endothermal peak appears with a large area. The disappearance of the peak indicates $S_1 = S_2$ at T_c. In other words, near T_c, both G curves may overlap within a small temperature range (but not at a particular point). The phase transition as such may be a higher order of transition.

As Ballman *et al.* [4] reported, the volume change of BNN is large at T_c, which is due to the large change in c-axis length. Therefore, the volume change will be detectable as the DSC endothermal peak at T_c. Here, the use of a sensitive sensor is desirable; in our experiments, a K-type sensor was used instead of an R-type sensor.

In our case, a relative comparison of volume change (and so ΔH_c) among the samples is of interest. Therefore, the DSC peak area can be an indicator of the magnitude of volume change. All samples have the same tungsten bronze-type of structure and certain elements (i.e. Ba, Na, Gd, Nb, O); the atomic ratio of Nb/O = 10/30 is kept constant and only the atomic

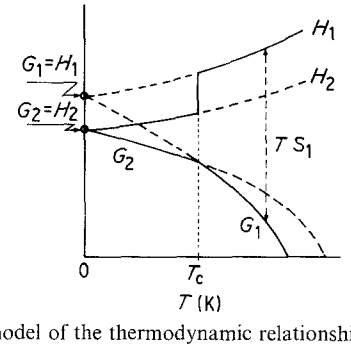

Figure 7 A model of the thermodynamic relationship of the phase transition.

ratio of Ba/Na/Ga varies between the samples. Therefore, the DSC indicator method should be effective for comparison of volume change at T_c. In fact, this method has proved successful as already described in Section 2.

The framework constructed with NbO_6 octahedra is strongly combined at the *ab*-axes plane level and its chemical bonds are not broken even at T_c. It is natural, consequently, that the change in *a*-axis at T_c is relatively small. On the other hand, the sites of the "open" tunnel parallel to the *c*-axis are occupied by barium, sodium and gadolinium. Therefore the *c*-axis at T_c changes distinctly with the ratio Ba/Na/Gd.

The electron configuration of the isolated Gd^{3+} ion is [Xe] $4f^7$, indicating the presence of a lone-pair electron. Therefore the bond strength of Gd–O may be stronger than that of Ba–O or Na–O, and the increase in gadolinium content may lead to the supression of volume change at T_c. However, this speculation contains may questionable factors, because it does not explain any thermal vibration of the lattice.

A more useful concept is that the other lanthanide ions are also possibly effective in suppressing the volume change at T_c, because they have similar ionic radii.

4. Conclusion

For samples of $Ba_{3+x}Na_{1+x}Gd_{1-x}Nb_{10}O_{30}$ ($1 \geqslant x \geqslant 0$) having a tungsten bronze-type of structure, the thermal volume change at the ferroelectric phase transition temperature (T_c) decreased with increasing gadolinium content or of Gd/(Ba + Na) ratio. This suggests that the addition of gadolinium or other lanthanide elements to $Ba_4Na_2Nb_{10}O_{30}$ may possibly be effective in obtaining an uncracked single crystal by the Czochralski technique, because the large thermal volume change at T_c causes the crystal to crack and this can be suppressed by the addition of, for example, gadolinium. However, colouring elements should be avoided if the application to the optically second harmonic generation (SHG) effect is required.

The DSC indicator method is useful in determining the relative magnitude of volume change at T_c for the sample series with similar compositions, which have the same type of structure and the same species of atoms with different atomic ratios. The reason for this was discussed from the thermodynamic viewpoint.

References

1. P. B. JAMIESON, S. C. ABRAHAMS and J. L. BERNSTEIN, *J. Chem. Phys.* **50** (1969) 4352.
2. L. G. VAN UITERT, J. J. RUBIN and W. A. BONNER, *IEEE J. Quant. Elect.* **QE4** (1968) 622.
3. A. W. VERE *et al.*, *J. Mater. Sci.* **4** (1969) 1075.
4. A. A. BALLMAN, J. R. CARRUTHERS and H. M. O'BRYAN Jr, *J. Cryst. Growth* **6** (1970) 184.
5. S. SINGH, D. A. DRAEGERT and J. E. GEUSIC, *Phys. Rev.* **B2** (1970) 2709.
6. T. YAMADA, H. IWASAKI and N. NIIZEKI, *J. Appl. Phys.* **41** (1970) 4141.
7. J. S. ABELL *et al.*, *J. Mater. Sci.* **6** (1971) 1084.
8. LANDOLT-BÖRNSTEIN,"Ferroelectrics and Related Substances" III/16 (Springer-Verlag, 1981) p. 179.
9. C. MANOLIKAS, *Ferroelectrics* **34** (1981) 235.
10. J. SCHNECK and F. DENOYER, *Phys. Rev.* **B23** (1981) 383.
11. J. SCHNECK *et al.*, *ibid.* **B25** (1982) 1766.
12. J. SCHNECK, G. CALVARIN and J. M. KIAT, *Amer. Phys. Soc.* (*Rapid Commun.*) (1984) 1476.
13. Y. UESU *et al.*, *Jpn J. Appl. Phys.* **27** (1988) 1167.
14. J. L. MUKHERJEE *et al.*, *J. Solid State Chem.* **24** (1978) 163.
15. M. W. CHASE Jr *et al.*, "JANAF Thermochemical Tables", 3rd Edn), Part II, Vol. 14, Suppl. 1 (National Bureau of Standards, Washington, 1985).
16. R. D. SHANNON and C. T. PREWITT, *Acta Crystallogr.* **B25** (1969) 925.
17. M. SHIMAZU, *et al.*, *Powder Diffraction* (to be published 1990).

Received 12 May
and accepted 20 October 1989